Accepted manuscript doi:
10.1680/jgele.20.00009

Accepted manuscript doi:
10.1680/jgele.20.00009

Submitted: 29 January 2020

Published online in 'accepted manuscript' format: 23 April 2020

Manuscript title: Mechanical behaviour of low-medium density destructured White Chalk

Authors: F. Alvarez-Borges*, B. N. Madhusudhan[†] and D. Richards[†]

Affiliations: *Diamond Light Source, Didcot, UK and [†]Faculty of Engineering and Physical Sciences, University of Southampton, Southampton, UK

Corresponding author: F. Alvarez-Borges, Beamline I12-JEEP, Diamond Light Source Ltd, Diamond House, Harwell Science and Innovation Campus, Didcot, Oxfordshire, OX11 0DE, UK. Tel.: +44 (0) 1235 777 528.

E-mail: fernando.alvarez-borges@diamond.ac.uk

Accepted manuscript doi:
10.1680/jgele.20.00009

Abstract

Low and medium density White Chalk often destructures during civil engineering works, forming a putty that exhibits problematic low-strengths in the short-term but may build-up strength with time. The underlying mechanisms that control the mechanical performance of the material are not well understood. This paper explores the prospect of developing a framework to characterise the behaviour of chalk putty. To this end, triaxial tests were carried out using low and medium density reconstituted chalks produced by different methods. Using void ratio vs mean effective stress results, a unique critical state line (CSL) is proposed, regardless of parent rock origin or the crushing process used to generate the putty material. The CSL was also found to satisfactorily fit independent test data by various authors, even though each independent sample material may have had different 'intrinsic' CSLs. This was suggested to stem from the similar particle characteristics of the chalks used. An assessment of the ageing effect indicates increases in strength as a result of densification due to consolidation and secondary compression, however, the end of test state could still be described using the CSL.

Keywords: Chalk; soft rocks; calcareous soils; silts; shear strength; time dependence

Accepted manuscript doi:
10.1680/jgele.20.00009

Civil engineering works in low and medium density Chalk often mechanically destructure the material, forming a putty-like mixture of whole and broken coccoliths (Lake, 1975; Clayton, 1978). This 'chalk putty' exhibits low strengths in the short-term but may build-up strength with time (Bialowas et al., 2018). Chalk putty may be encountered at the interface between foundation elements and the Chalk formation, like the chalk putty 'annulus' formed around driven piles upon installation (Hobbs and Atkinson, 1993; Lord et al., 2002). In these cases, foundation capacity may be dependent on the strength of chalk putty, but there is limited knowledge of its mechanical behaviour. However, there is evidence that destructured chalk is principally a silt and clay-sized largely non-plastic granular material (Clayton, 1983; Razoaki, 2000; Doughty, 2016; Bialowas, 2017), and it can be reasonably expected that its failure states are described by critical state concepts (Leddra, 1989; Burland, 1990a; Leddra and Jones, 1990; Lord et al., 1994). However, previous critical state characterisation efforts have yielded multiple critical state lines suitable to specific material characteristics and testing conditions (e.g. Bialowas & Diambra, 2018; Doughty et al., 2018; Alvarez-Borges et al., 2018b). From this perspective, this Letter presents a laboratory investigation on destructured low-medium density White Chalk aimed at examining the suitability of a critical state framework to describe its mechanical behaviour.

Materials and methods

Destructured chalk preparation

Intact chalk samples were collected at two sites in southern England: Somborne Chalk Quarry (SOM) in Hampshire, and a quarry near St. Nicholas-at-Wade (SNW), in Kent. The samples were extracted from the Newhaven and Margate Chalk formations, respectively. Additional sampling site information is available in Alvarez-Borges (2014), Bialowas (2017) and Buckley et al. (2018).

Accepted manuscript doi:
10.1680/jgele.20.00009

Two different destructuration methods were applied to each of the intact chalk samples. Method A comprised the use of a food (cheese) grater to disaggregate oven-dried blocks about 5 cm in diameter, whilst method B involved the use of a manual food grinder (meat mincer) to crush saturated gravel-sized lumps. Dry and wet sieving through the 425 μm mesh was applied to the product of methods A and B, respectively. The material from both methods was stored wet in sealed bags for about four weeks prior to specimen preparation, to promote $CaCO_3$ dissolution, as discussed by Bialowas (2017).

The use of these preparation procedures was expected to enable the comparison with consolidation data reported by Alvarez-Borges et al. (2018a), and to facilitate the assessment of the influence of the preparation method and material origin on the characteristics and shearing behaviour of chalk putty (Cuccovillo and Coop, 1993; Vaughan, 1997). Index properties were determined in accordance to BS 1377-2:1990 (BSI, 1998b) and BS-ISO 13320:2009 (BS-ISO, 2009) and are listed in Table 1. Particle size distribution (PSD) curves are given in Fig. 1. Scanning electron microscopy (SEM) images of the intact and destructured materials are shown in Fig. 2.

Triaxial tests

Consolidated undrained triaxial tests were conducted using a standard triaxial apparatus, as detailed in BS 1377-8:1990 (BSI, 1998a). Pore water pressure (u) transducers were connected to the top and bottom specimen drainage lines, and cell and back pressure were applied via digital pressure controllers. Specimens were 38mm in diameter and 76mm high and were locally instrumented with a submersible linear variable differential transformer (LVDT) to measure radial strain. Global axial displacements were measured via an externally mounted LVDT; axial loads were determined using a submersible load cell.

Specimens were prepared using chalk putty at water contents (*w*) between 1 and 1.5 times the liquid limit, as advised by Burland (1990b). Excess water was removed from the sample bags prior to specimen preparation and used to fill the back pressure controller. The putty was thereafter transferred to a vacuum chamber for minimum 2h and then used to fill a split-former assembled on the pedestal of the triaxial cell. The material was placed using a small spatula and gently stirred with a glass rod to remove air bubbles, as described by Doughty (2016). A small pre-consolidation stress (≈7 kPa) was applied before removing the split former, to avoid large pre-test distortions. Back pressures between 300 and 400 kPa were then applied to achieve saturation B-values of about 0.95. Specimens were thereafter consolidated in isotropic (ISO) or one-dimensional (1D) fashion to targeted mean effective stress levels to attain pre-shear conditions qualitatively representative of 'loose' and 'dense' states. Consolidation stress levels and top-bottom drainage were maintained during varied time periods until axial creep rates reduced to less than about 0.003 %/h (after Kuwano and Jardine, 2002). Additionally, Test 6 was maintained under constant p' in drained conditions for 13 days to investigate potential time-based gains in strength. All specimens were then sheared under strain-control. Pre- and post-test specimen weight, *w* and volume were used to derive in-test void ratios (*e*), as detailed by Madhusudhan and Baudet (2014), using a specific gravity of 2.70, after Clayton (1983). Specimen details are presented in Table 2.

Results

Fig. 3 depicts stress paths in q – p' space (a), and q – axial strain (ε_{ax}) and (b) u - ε_{ax} data (c). Most specimens exhibited contractive behaviour and effective stress reductions after yielding until reaching phase transformation (Ishihara et al., 1975), followed by a dilative response. As is often the case during triaxial testing involving standard porous end platens, strain localisation in the form of multiple conjugate shear bands was observed (Desrues and Ando,

2015; Salvatore et al., 2017). The effect of strain localisation may be noted as a final stress path reversal from dilating to contracting in Fig. 3a (Burland, 1990b), and might have led to a modest underestimation of ultimate strengths (Lee, 1976). 'End of test' states are denoted by markers before this reversal. The term 'end of state' is preferred over 'critical state' because, in some cases, strain localisation prevented the attainment of global theoretical critical state conditions (i.e. shearing at constant p', q and *e*; Roscoe et al, 1958). This is indicated in Table 2. It is acknowledged that strain localisation may have commenced before being detectable from global stress/strain measurements.

Fig. 4 presents end of test states and stress paths in *e* – ln p' space for all triaxial tests.

Despite the limitations of strain localisation, a unique non-linear CSL may be proposed:

$$e = 0.895 - 0.071(\mathrm{p}'/\mathrm{p}'_{\mathrm{ref}})^{0.186} \quad (1)$$

where $\mathrm{p}'_{\mathrm{ref}}$ = 1 kPa for dimensional consistency. Curved CSLs in *e* – ln p' space are typical for many non-cohesive soils (Li and Wang, 1998), though they are sometimes represented as linear for simplicity (Been et al., 1991).

The average critical state stress ratio q/p' = M derived from tests that globally appeared to reach critical state conditions was 1.36, equivalent to a critical state angle of friction (ϕ'_c) of 33.7°, which is comparable to previously reported values (30-35°; Clayton, 1978; Razoaki, 2000; Doughty, 2016; Bialowas, 2017).

Accepted manuscript doi:
10.1680/jgele.20.00009

Discussion

General mechanical behaviour of chalk putty

As for many sands, shearing behaviour appears to be substantially affected by pre-shear density. Specimens reconstituted at states 'loose' of the proposed CSL predominantly exhibited contractive behaviour upon shearing (Tests 6, 7, 8 and 9 in Figs. 3-4), developing positive *u* values. Conversely, dilative behaviours were encountered in dry side of critical experiments (Tests 1, 2, 4 and 10 in Figs. 3-4), with negative *u* developments being predominant.

The proposed CSL (Eq. (1)) runs parallel to the 1D-NCL proposed by Alvarez-Borges et al. (2018a):

$$e = 0.928 - 0.071(\mathrm{p}'/\mathrm{p}'_{\mathrm{ref}})^{0.186} \quad (2)$$

The suitability of these parallel state curves to characterise compression and shear behaviours suggests that the mechanical performance of chalk putty is not fundamentally different to that of monomineralic uniform sands (e.g. Coop & Lee, 1993; Verdugo & Ishihara, 1996). As for these materials, the location of these curves in volumetric space is likely dependent on material characteristics such as PSD, particle shape, mineralogy, etc. The parent low-medium density White Chalk rocks used were largely composed by calcareous coccolithic debris, and Fig. 2 evidences that the destructuration methods employed mainly entailed the disaggregation of these constitutive particles. This yielded putties with limited differences in PSD (Fig. 1), particle shape (Fig. 2) and mineralogy (Table 1), which explains the suitability of a single CSL for these materials.

Accepted manuscript doi:
10.1680/jgele.20.00009

Chalk putty origin and the Critical State Line

Considering the suitability of a unique CSL to describe the failure states of the four tested putties, it may be postulated that putties created from similar parent intact chalks also have comparable particle characteristics and have a similar CSL. To examine this, end of test triaxial data by Clayton (1978), Doughty (2016) and Bialowas (2017) have been plotted in Fig. 5 alongside the results presented before. Ultimate state void ratios in the dataset by Doughty (2016) correspond to those recorded upon specimen removal by the same author, which were felt to better reflect the global void ratio during shear. Sample details and end of test data are presented in Table 3 and Table 4.

Fig. 5 evidences that the proposed CSL is a reasonable fit to the independent test data, even though each material had a different intrinsic CSL appropriate to their PSD. Such applicability of a single CSL to independent datasets is not encountered elsewhere in the Chalk literature. It is apparent that the underlying phenomena that controls the ultimate strength-volumetric state relationship of chalk putty are not substantially affected by the procedure used to crush the chalk, the variability of the parent low-medium density rock, the lower p' range used, or the differences in overall particle size distribution (Fig. 6a). This is probably because low-medium density White Chalk *fines* exhibit limited differences in particle shapes and sizes (Fig. 6b), and this *fine fraction* controls the mechanical performance of crushed White Chalk when it accounts for at least 20% of its dry weight (Puig, 1973; Rat and Schaeffner, 1990). Though some degree of grain breakage may have occurred during shear, the coarser fraction likely broke down into fines of similar characteristics to those tested in this study, while the fine fraction is expected to have exhibited limited comminution at the moderate stress levels used (see Alvarez-Borges et al., 2018a). In any event, particle breakage during shear seems to have been insufficient to significantly alter the suitability of

the CSL in the compression plane. However, it must be emphasised that different particle characteristics introduced by diagenesis or destructuration may affect the observed behaviour. For instance, it is not expected that partially destructured chalk containing mostly coarse particles, crushed chalks produced from high IDD rocks containing significant proportions of authigenic calcite grains, and materials containing important amounts of non-calcite minerals will share the same CSL given above.

Effect of ageing on the ultimate strength of chalk putty

Fig. 3 and Fig. 4 present results for Tests 6, 7 and 9 which were sheared at broadly similar void ratios, but aged for 13, 1.8 and 3.6 days, in each case. Comparable end of test strengths consistent with the CSL are evident, regardless of whether the pre-shear p' - *e* conditions were attained by prolonged ageing or by subjecting an initially denser specimen to lower p' levels and/or a shorter consolidation period. Similar behaviour is observed using independent data from Doughty (2016) and Bialowas (2017), shown in Fig. 7 (Table 4). This Figure denotes that ultimate states are not affected even by several weeks of drained ageing and considerably different pre-shear p' levels, and are instead dependent on the pre-shear void ratio. It is also evident from Fig. 3a and Fig. 7 that ageing does not affect the magnitude of ϕ'_c. These observations are consistent with the data presented in Fig. 5, which includes results from drained and undrained triaxial experiments involving various ageing periods (Table 4) and demonstrate for the first time that ageing does not alter the location of the CSL. This implies that any re-cementation by $CaCO_3$ precipitation during ageing is largely broken down during shearing and does not modify critical state parameters. Thus, the impact of chemically-induced ageing is probably limited to small strain behaviour, as discussed by Bialowas (2017).

Accepted manuscript doi:
10.1680/jgele.20.00009

To explain improvements in large-strain chalk putty strength associated with ageing, Fig. 8a presents the volumetric compression path of Test 6, where reductions in void ratio whilst ageing at constant p' are evident. These void ratio reductions can be associated with an increment of the equivalent p' on the CSL at the current void ratio (p'_c) of over 100%, which may be linked with a similar increase in strength. Fig. 8b shows that a significant portion of p'_c increments in the time domain occur when the reduction in void ratio becomes approximately linear with the logarithm of time ($\Delta e/\Delta \log t = C_\alpha$), a mechanism commonly interpreted as secondary compression (Mesri, 1973). It may be thus proposed that volumetric strains occurring during and after the end of primary compression result in an increment in ultimate strength compatible with the decrease in void ratio, and that these strains are a potential cause of the ageing or long-term 'strengthening' of destructured chalk.

Conclusions

A series of undrained triaxial experiments reveal a unique critical state line (CSL) for reconstituted White Chalk produced by two different methods from low-medium density parent rocks sampled from two locations. The underlying reason for the uniqueness of the CSL was proposed to be that the materials were largely constituted by coccolithic debris and exhibited a similar particle size distribution (PSD). The proposed CSL was also found to be a reasonable fit for independent test data involving crushed chalks largely composed by fines and produced from similar chalk rocks, but exhibiting different PSDs. Chalk putty ageing was not observed to alter the suitability of the CSL, and ageing-related strength gains were proposed to be explained by void ratio reductions driven by consolidation and secondary compression. Overall, results support the use of the proposed CSL to characterise the general mechanical behaviour of the material, without disputing the fact that different intrinsic CSLs exist for materials of different PSD.

Acknowledgements

This research has been co-sponsored by the National Council of Science and Technology (CONACyT) of Mexico, and by the Faculty of Engineering and Physical Sciences of the University of Southampton.

List of notation

C_α	Coefficient of secondary compression
e	Void ratio
IDD	Intact dry density
K_0	Ratio of vertical to radial effective stress in vertical zero-radial strain compression
M	Ratio between q and p' at critical state
p'	Mean effective stress: $(\sigma'_1 + \sigma'_2 + \sigma'_3)/3$
p'_c	Mean effective stress on the critical state line at current void ratio.
p'_{ref}	Reference mean effective stress = 1 kPa
q	Deviator stress. In in triaxial tests = $\sigma'_1 - \sigma'_3$
u	Pore water pressure
w	Water content
ε_{ax}	Axial strain in triaxial tests.
σ'_1	Major principal stress
σ'_2	Intermediate principal stress
σ'_3	Minor principal stress
ϕ'_c	Critical state angle of friction

Accepted manuscript doi:
10.1680/jgele.20.00009

References

Alvarez-Borges F.J. (2014) *The application of simple shear testing to evaluate the shaft resistance on piles driven in chalk.* MSc Dissertation, University of Southampton, Southampton, UK.

Alvarez-Borges F.J., Madhusudhan B.N. and Richards D.J. (2018a) The 1D normal compression line and structure permitted space of low-medium density chalk. *Geotech Lett* 8, No. 4, 298-304. doi: 10.1680/jgele.18.00091.

Alvarez-Borges F.J., Clayton C.R.I., Richards D.J. and Madhusudhan B.N. (2018b) The effect of the remoulded void ratio on unit shaft friction in small-displacement piles in chalk. In: *Engineering in Chalk, Proceedings of the Chalk 2018 Conference* (Lawrence J., Preene M., Lawrence U. and Buckley R.M. (eds)). ICE Publishing, 475-480. doi: 10.1680/eiccf.64072.475

Been K., Jefferies M.G. and Hachey J. (1991) The critical state of sands. *Géotechnique* 41, No. 3, 365-381. doi: 10.1680/geot.1991.41.3.365.

Bialowas G. (2017) *Time and Stress Dependent Mechanical Properties of Reconstituted Chalk.* PhD Thesis, University of Bristol, Bristol, UK.

Bialowas G. and Diambra A. (2018) Time and stress dependent strength and stiffness of reconstituted chalk. In: *Engineering in Chalk, Proceedings of the Chalk 2018 Conference* (Lawrence J., Preene M., Lawrence U. and Buckley R.M. (eds)). ICE Publishing, 503-508. doi: 10.1680/eiccf.64072.503.

Bialowas G.A., Diambra A. and Nash D.F.T. (2018) Stress and time-dependent properties of crushed chalk. *P I Civil Eng-Geotec* 171, No. 6, 530-544. doi: 10.1680/jgeen.17.00168.

BS-ISO (2009) 13320:2009. Particle size analysis - Laser diffraction methods. British Standards Institution, London, UK.

BSI (1998a) 1377-8:1990. Methods of tests for soils for civil engineering purposes - Part 8: Shear strength tests (effective stress). British Standards Institution (BSI), London (UK).

BSI (1998b) 1377-2:1990. Methods of test for soils for civil engineering purposes - Part 2: Classification tests. British Standards Institution (BSI), London, UK.

Buckley R.M., Jardine R.J., Kontoe S. and Lehane B.M. (2018) Effective stress regime around a jacked steel pile during installation ageing and load testing in chalk. *Can Geotech J* 55, No. 11, 1577-1591. doi: 10.1139/cgj-2017-0145

Burland J.B. (1990a) Preface. In: *Chalk: Proceedings of the International Chalk Symposium* (Burland J.B., Mortimore R.N., Roberts L.D., Jones D.L. and Corbett B.O. (eds)). Thomas Telford, London, UK, 1-4.

Burland J.B. (1990b) On the compressibility and shear strength of natural clays, The 30th Rankine Lecture. *Géotechnique* 40, No. 3, 329-378. doi: 10.1680/geot.1990.40.3.329.

Clayton C.R.I. (1978) *Chalk as fill.* PhD Thesis, University of Surrey, Guildford, UK.

Clayton C.R.I. (1983) The Influence of Diagenesis on Some Index Properties of Chalk in England. *Géotechnique* 33, No. 3, 225-241. doi: 10.1680/geot.1983.33.3.225.

Coop M.R. and Lee I.K. (1993) The behaviour of granular soils at elevated stresses. In: *Predictive Soil Mechanics, Proceedings of the Wroth Memorial Symposium* (Houlsby G.T. and Schofield A. (eds)). Thomas Telford, London, UK, 186-198.

Cuccovillo T. and Coop M.R. (1993) The influence of bond strength on the mechanics of carbonate soft rocks. In: *Proceedings of an International Symposium on Geotechnical Engineering of Hard Soils - Soft Rocks* (Anagnostopoulos A., Schlosser F., Kalteziotis N. and Frank R. (eds)). AA Balkema, Rotterdam, NL, Vol 1, 447-455.

Desrues J. and Ando E. (2015) Strain localisation in granular media. *Cr Phys* 16, No. 1, 26-36. doi: 10.1016/j.crhy.2015.01.001.

Doughty L. (2016) *Laboratory Testing of Chalk.* MSc Dissertation, Imperial College London, London, UK.

Doughty L., Buckley R.M. and Jardine R.J. (2018) Investigating the effect of ageing on the behaviour of chalk putty. In: *Engineering in Chalk, Proceedings of the Chalk 2018 Conference* (Lawrence J., Preene M., Lawrence U. and Buckley R.M. (eds)). ICE Publishing, 695-701. doi: 10.1680/eiccf.64072.695.

Hancock J.M. (1975) The petrology of chalk. *P Geologist Assoc* 86, No. 4, 499-535. doi: 10.1016/S0016-7878(75)80061-7.

Hobbs N.B. and Atkinson M.S. (1993) Compression and tension tests on an open ended tube pile in chalk. *Ground Engineering* 26, No. 3, 30-34.

Ishihara K., Tatsuoka F. and Yasua S. (1975) Undrained deformation and liquefaction of sand under cyclic stresses. *Soils Found* 15, No. 1, 29-44. doi: 10.3208/sandf1972.15.29.

Kuwano R. and Jardine R.J. (2002) On measuring creep behaviour in granular materials through triaxial testing. *Can Geotech J* 39, No. 5, 1061-1074. doi: 10.1139/T02-059.

Lake L.M. (1975) *Engineering Properties of Chalk with Special Reference to Foundation Design and Performance.* PhD Thesis, University of Surrey, Guilford, UK.

Leddra M.J. (1989) *Deformation of chalk through compaction and flow.* PhD Thesis, University of London (University College London), London, UK.

Leddra M.J. and Jones M.E. (1990) Steady-state flow during undrained loading of chalk. In: *Chalk: Proceedings of the International Chalk Symposium* (Burland J.B., Mortimore R.N., Roberts L.D., Jones D.L. and Corbett B.O. (eds)). Thomas Telford Ltd, London, UK, 245-252.

Lee K.L. (1976) Influence of end restraint in cyclic triaxial tests. Vicksburg, MS, USA: United States Department of Defense.

Li X.S. and Wang Y. (1998) Linear representation of steady-state line for sand. *J Geotech Geoenviron* 124, No. 12, 1215-1217. doi: 10.1061/(Asce)1090-0241(1998)124:12(1215).

Lord J.A., Twine D.P. and Yeow H. (1994) *CIRIA Project Report 11: Foundations in chalk*, Construction Industry Research and Information Association (CIRIA), London, UK.

Lord J.A., Clayton C.R.I. and Mortimore R.N. (2002) *CIRIA Report C 574: Engineering in Chalk*, Construction Industry Research and Information Association (CIRIA), London, UK.

Madhusudhan B.N. and Baudet B.A. (2014) Influence of reconstitution method on the behaviour of completely decomposed granite. *Géotechnique* 64, No. 7, 540-550. doi: 10.1680/geot.13.P.159.

Mesri G. (1973) Coefficient of Secondary Compression. *J Soil Mech Found-Asce* 99, No. 1, 123-137.

Puig J. (1973) Problemes de terrassement dans la craie. *Bull. Liaison Labo. P. et Ch.* 63, No. 1, 56-72.

Rat M. and Schaeffner M. (1990) Classification of chalks and conditions of use in embankments. In: *Chalk: Proceedings of the International Chalk Symposium* (Burland J.B., Mortimore R.N., Roberts L.D., Jones D.L. and Corbett B.O. (eds)). Thomas Telford, London, UK, 425-428.

Razoaki R.N. (2000) *Effect of ageing on mechanics of chalk slurries.* PhD Thesis, University of Portsmouth, Portsmouth, UK.

Roscoe K.H., Schofield A.N. and Wroth C.P. (1958) On The Yielding of Soils. *Géotechnique* 8, No. 1, 22-52. doi: 10.1680/geot.1958.8.1.22.

Salvatore E., Modoni G., Ando E., Albano M. and Viggiani G. (2017) Determination of the critical state of granular materials with triaxial tests. *Soils Found* 57, No. 5, 733-744. doi: 10.1016/j.sandf.2017.08.005.

Vaughan P.R. (1997) Engineering behaviour of weak rocks: Some answers and some questions. In: *Proceedings of an International Symposium on Geotechnical Engineering of Hard Soils - Soft Rocks* (Anagnostopoulos A., Schlosser F., Kalteziotis N. and Frank R. (eds)). AA Balkema, Rotterdam, NL, Vol 3, 1741-1765.

Verdugo R. and Ishihara K. (1996) The steady state of sandy soils. *Soils Found* 36, No. 2, 81-91. doi: 10.3208/sandf.36.2_81.

Accepted manuscript doi:
10.1680/jgele.20.00009

Table 1. Sample index parameters (intact chalk data shown in italics).

	SNW-A	SNW-B	SOM-A	SOM-B
Formation	*Seaford*	*Seaford*	*Newhaven*	*Newhaven*
*Mean IDD (Mg/m^3)**	*1.57 ±0.08*	*1.57 ±0.08*	*1.47 ±0.08*	*1.47 ±0.08*
$CaCO_3$ content (%)**	≈98.2	≈98.2	≈98.5	≈98.5
Crushing method	A	B	A	B
Liquid limit (%)	29	28	30	31
Plastic limit (%)	22	22	23	22
d_{50} (μm)	4.8	4.9	5.4	4.7
d_{10} (μm)	1.4	1.4	1.5	1.5
d_{60}/d_{10}	5.1	4.8	5.0	4.3

* IDD = Intact dry density; measured using gas jar method by Clayton (1983).
** Based on Hancock (1975).

Table 2. Triaxial test details.

Test No.	Prep. Details	Pre-shear conditions p' (kPa)	q (kPa)	e	Ageing (days)	Shear rate (%/h)	CS†	Ultimate state p'‡ (kPa)	q‡ (kPa)	φ' (°)
1	SNW-B	1762	1396	0.571	<1	0.1	No	2894	4318	36.7
2	SNW-B	1879	1648	0.585	<1	0.2	No	2523	3696	36.1
3	SNW-B	52	1	0.743	1.7	0.2	Yes	61	85	34.4
4	SNW-B	268	16	0.674	<1	0.2	Yes	515	726	34.8
5	SNW-B	1301	2	0.630	1.1	0.2	No	1228	1644	33.2
6	SNW-B	1306	3	0.670	13	0.2	Yes	713	983	34.1
7	SNW-A	805	2	0.658	1.8	0.2	Yes	649	821	31.5
8	SOM-B	1904	1815	0.629	3.7	0.2	No	1502	2029	33.5
9	SOM-B	1299	2	0.659	3.6	0.2	Yes	685	914	33.1
10	SOM-A	1295	3	0.594	3.2	0.2	Yes	2057	2877	34.6

† Critical State: Yes = constant p' and q attained before visible strain localisation; No = constant p' and q not attained at end of test.
‡ $p' = (\sigma'_1 + \sigma'_2 + \sigma'_3)/3$ (mean effective stress) and $q = \sigma'_1 - \sigma'_3$ (deviator stress), where σ'_1, σ'_2, σ'_3 are the principal effective stresses as customary.

Accepted manuscript doi:
10.1680/jgele.20.00009

Table 3. Chalk putty index properties according to various researchers.

Author	Sample name	Sampling location	Formation	Mean IDD (Mg/m^3)	Prep. method	Grading range	LL (%)	PL (%)
Clayton (1978)*	4C	Swanley	Seaford	1.43	Oven-dry crushed	<2 mm	n/a	n/a
Doughty (2016)‡	D	Wikinger	Maastrichtian	1.50	Saturated-crushed	Unrestr.†	33 to 38	23 to 25
Bialowas (2017)	B	St. Nicholas-at-Wade	Margate	n/a	Oven-dry crushed	Unrestr.†	30	22

Note: see text for preparation method details.
* Old lithostratigraphy used by original author.
† 'Unrestricted grading', i.e. no sieving treatment was applied.
‡ Some material data obtained from Doughty et al. (2018).

Accepted manuscript doi:
10.1680/jgele.20.00009

Table 4. Independent end of test triaxial data shown in Fig. 5.

Author	Sample name	Ageing (days)	Shearing conditions	p' (kPa)	e
Clayton (1978)	4C	<1	Undrained	42	0.747
	4C	<1	Undrained	64	0.738
	4C	<1	Undrained	85	0.746
	4C	<1	Undrained	128	0.707
	4C	<1	Undrained	179	0.714
	4C	<1	Undrained	169	0.737
	4C	16	Undrained	168	0.701
	4C	16	Undrained	256	0.684
	4C	16	Undrained	340	0.692
	4C	20	Undrained	142	0.700
	4C	20	Undrained	236	0.682
	4C	20	Undrained	365	0.682
	4C	37	Undrained	202	0.677
	4C	37	Undrained	294	0.680
	4C	37	Undrained	466	0.660
Doughty (2016)	D	<1	Undrained	23	0.754
	D	7	Undrained	138	0.726
	D	7	Undrained	603	0.645
	D	14	Undrained	344	0.670
Bialowas (2017)	B	1	Drained	535	0.687
	B	3	Drained	184	0.704
	B	3	Drained	200	0.695
	B	4	Drained	542	0.688
	B	4	Drained	548	0.682
	B	5	Drained	358	0.700
	B	5	Drained	353	0.687
	B	6	Drained	535	0.690
	B	15	Drained	568	0.661
	B	26	Drained	343	0.690
	B	27	Drained	362	0.694
	B	65	Drained	546	0.700
	B	4	Undrained	127	0.722
	B	5	Undrained	110	0.718
	B	58	Undrained	235	0.669
	B	69	Undrained	131	0.745

Accepted manuscript doi:
10.1680/jgele.20.00009

Figure captions

Fig. 1. Cumulative PSD curves of the four chalk putty samples.

Fig. 2. SEM micrographs (10000x) of intact (a) and destructured (b) SNW chalk (method B): 1 – intact coccolith; 2 – broken coccolith; 3 – coccolithic platelets; 4 – authigenic calcite grain.

Fig. 3. Triaxial test results: (a) stress paths; (b) lower stress range in (a); (c) stress – strain curves; (d) pore pressure evolution. Labels denote test number (Table 2).

Fig. 4. Undrained triaxial shearing paths and ultimate states in ln p' – e plane. Data labels denote test number (see Table 2).

Fig. 5. Comparison between end of test states from triaxial experiments by various authors (see Table 3 for legend key) and Tests 1 to 10 of this paper (SNW and SOM). Open and filled markers denote drained and undrained test data, respectively; crossed markers refer to short-term conditions.

Fig. 6. (a) Cumulative PSD curves of crushed chalks studied by Clayton (1978) and Bialowas (2017); Note that the curve for the former has no grading restriction (Table 3). (b) Cumulative PSD curves of crushed chalks with 425 μm upper size limit, from various authors.

Fig. 7. Undrained triaxial test data from Doughty (2016) and Bialowas (2017) after various ageing periods. End of test conditions interpreted from graphs by the original authors.

Fig. 8. (a) Volumetric compression path for Test 6; (b) Time-based decrease in e and increase in p'_c during final p' ramp and ageing period.

Accepted manuscript doi:
10.1680/jgele.20.00009

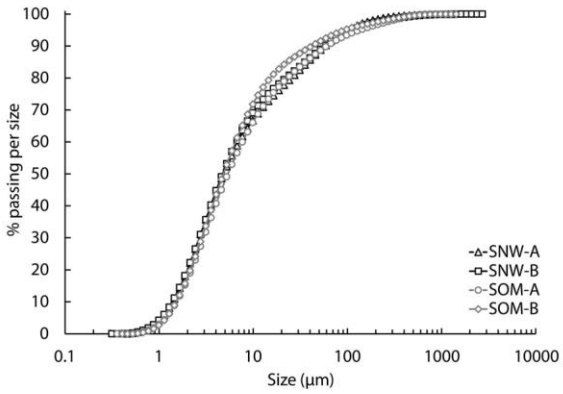

Fig01_rev2

Accepted manuscript doi:
10.1680/jgele.20.00009

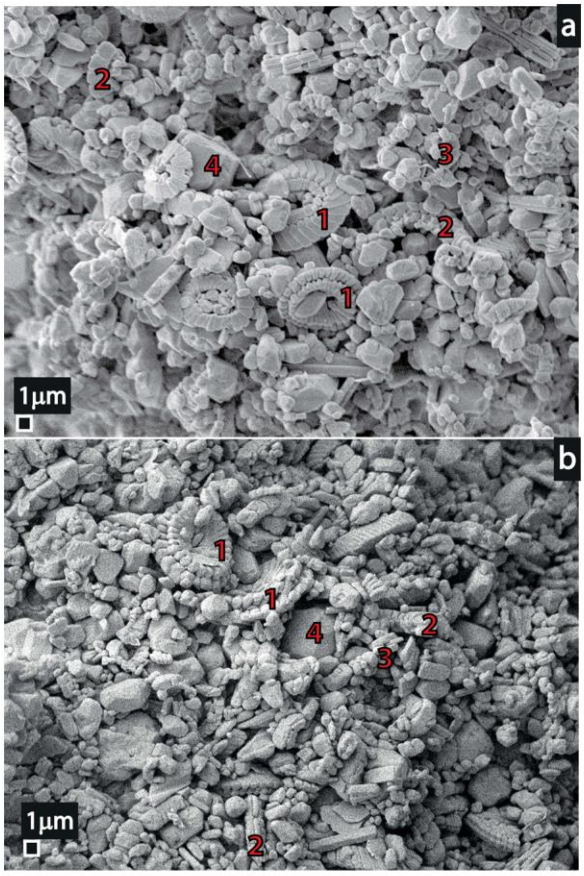

Fig02_rev2

Accepted manuscript doi:
10.1680/jgele.20.00009

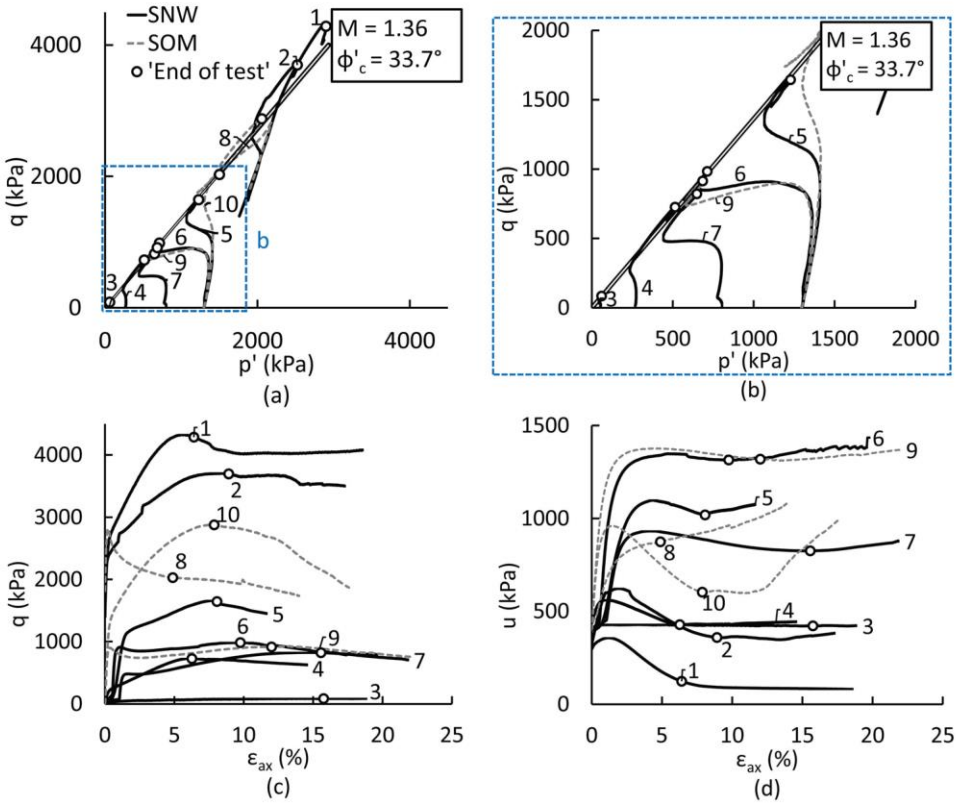

Fig03_rev2

Accepted manuscript doi:
10.1680/jgele.20.00009

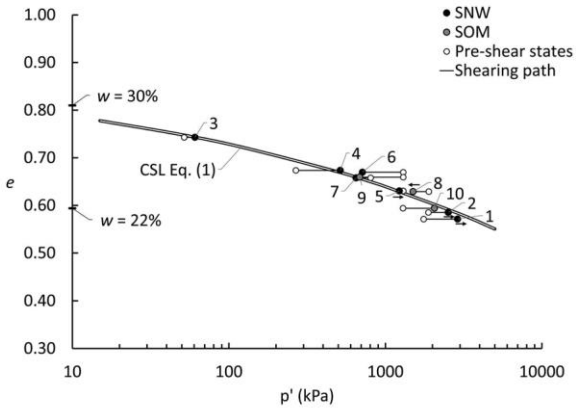

Fig04_rev2

Accepted manuscript doi:
10.1680/jgele.20.00009

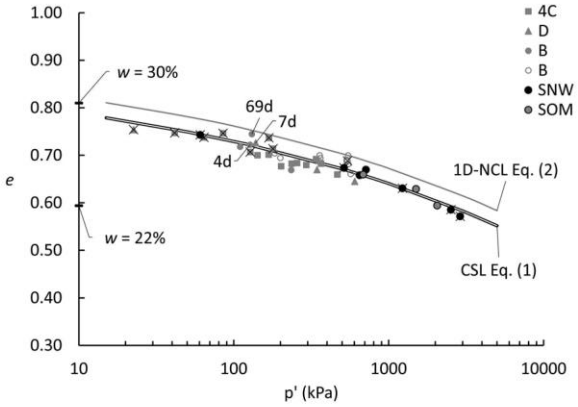

Fig05_rev2

Accepted manuscript doi:
10.1680/jgele.20.00009

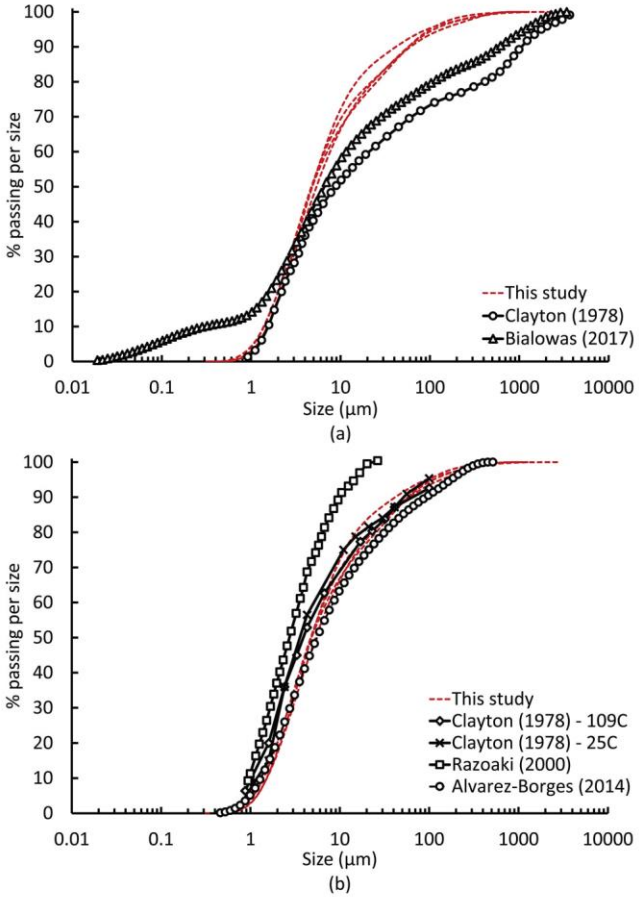

Fig06_rev2

Accepted manuscript doi:
10.1680/jgele.20.00009

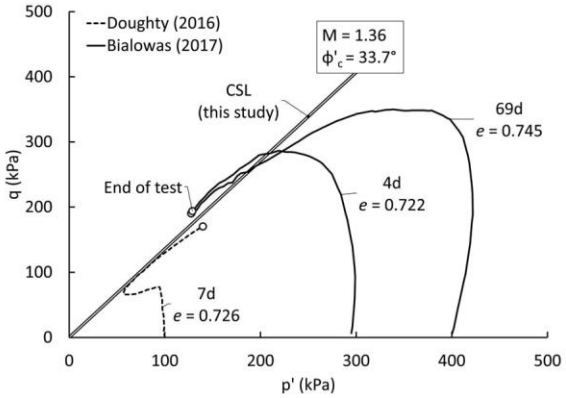

Fig07_rev2

Accepted manuscript doi:
10.1680/jgele.20.00009

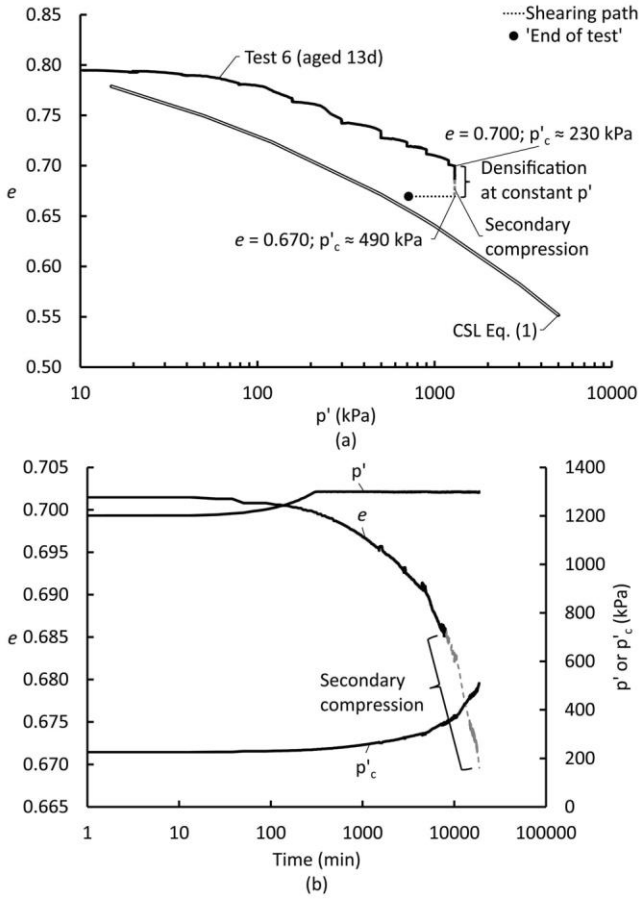

Fig08_rev2